CHIN. PHYS. LETT. Vol. 34, No. 4 (2017) 041201

Curvature of Pseudocritical Transition Line for Two-Flavor QCD with Improved Kogut–Susskind Quarks *

Liang-Kai Wu(吴良凯)[1**], Xiang-Fei Meng(孟祥飞)[2], Fa-Ling Zhang(张法玲)[1]
[1]Faculty of Science, Jiangsu University, Zhenjiang 212013
[2]National Supercomputer Center, Tianjin 300457

(Received 2 November 2016)

The results on the curvature of a pseudocritical transition line for two-flavor QCD through lattice simulations are presented. The simulations are carried out with Symanzik-improved gauge action and Asqtad fermion action on a lattice $12^3 \times 4$ at quark mass $am = 0.010$. At the imaginary chemical potentials $a\mu_{\rm I} = 0.050$, 0.150, 0.200, 0.225 and 0.250, we investigate the chiral condensate $\bar{\psi}\psi$, plaquette variable P and imaginary part of Polyakov loop $\mathrm{Im}(L)$ and their susceptibilities. Analytic continuation from an imaginary chemical potential to a real one is used to obtain the expression for transition temperature as a function of the chemical potential. The curvature is 0.0326(46).

PACS: 12.38.Gc, 11.10.Wx, 11.15.Ha, 12.38.Mh DOI: 10.1088/0256-307X/34/4/041201

The phase diagram of QCD has significant phenomenological implications. It is relevant to the early universe, compact stars and heavy ion collision experiments. Determining the phase diagram of QCD is the central goal of lattice QCD simulation. Despite great progress having been made theoretically and experimentally, the phase diagram of QCD remains a challenge for theoretic physics. Overviews may be found in Ref. [1] and references therein.

Heavy-ion collisions provide us with opportunities to probe the transition of QCD. In heavy-ion collisions, high-energy particles collide with each other and may generate fireballs which could fulfill the extreme conditions. Under such circumstances, the quark gluon plasma cools down quickly and the system freezes out into the hadrons and chemical elements. The transition takes place at a given collision energy, the locations of transition can be described in terms of two parameters, the freeze-out temperature T and the baryon density $\mu_{\rm B}$. On the T–$\mu_{\rm B}$ plane, the freeze-out temperature T at different baryon densities $\mu_{\rm B}$ forms a curve which is referred to as the pseudocritical transition line.[2]

Lattice QCD simulation at finite density encounters the problem of complex fermionic determinant for any $SU(3)$ gauge theory which prohibits importance sampling.[3] Different methods have been used to solve this complex action problem.[4,5] Among these methods, the imaginary chemical potential method is employed to carry out lattice QCD simulations.[6–13]

In this work, we aim to determine the curvature of the pseudocritical line of $N_{\rm f} = 2$ QCD with one-loop Symanzik-improved gauge action [14–17] and Asqtad KS action.[18,19] These actions have discretization error of $O(\alpha_{\rm s}^2 a^2, a^4)$ and $O(\alpha_{\rm s} a^2, a^4)$, respectively. These improvements are significant on $N_{\rm t} = 4$ lattice where the lattice spacing is quite large. Standard KS fermions suffer from taste symmetry breaking at nonzero lattice spacing a.[20] This taste symmetry breaking can be illustrated by the smallest pion mass taste splitting which is comparable to the pion mass even at lattice spacing $a \sim 0.1\,\mathrm{fm}$.[21] Asqtad KS action has good taste symmetry and free dispersion relation through introducing fattened links and the so-called 'Naik terms'.[22,23]

After introducing pseudofermion field Φ, the partition function of the system can be expressed as

$$Z = \int [dU][d\Phi^*][d\Phi] e^{-S_{\rm g} - S_{\rm f}},$$

where $S_{\rm g}$ is the Symanzik-improved gauge action, and $S_{\rm f}$ is the Asqtad quark action with the quark chemical potential μ. Here we take $\mu = i\mu_{\rm I}$ with $\mu_{\rm I}$ being a real number. For $S_{\rm g}$, we use

$$S_{\rm G} = \beta(C_P \sum_{x;\mu<\nu} (1 - P_{\mu\nu}) + C_R \sum_{x;\mu\neq\nu} (1 - R_{\mu\nu}) + C_T \sum_{x;\mu<\nu<\sigma} (1 - T_{\mu\nu\sigma})),$$

with $P_{\mu\nu}$, $R_{\mu\nu}$ and $T_{\mu\nu\sigma}$ standing for 1/3 of the imaginary part of the trace of 1×1, 1×2 planar Wilson loops and $1\times1\times1$ 'parallelogram' loops, respectively,

$$P_{\mu\nu} = \frac{1}{3}\mathrm{ReTr}$$

$$R_{\mu\nu} = \frac{1}{3}\mathrm{ReTr}$$

$$T_{\mu\nu\sigma} = \frac{1}{3}\mathrm{ReTr}$$

The coefficients C_P, C_R and C_T are tadpole improved,[21]

$$C_P = 1.0,$$
$$C_R = \frac{-1}{20u_0^2}(1 - (0.6264 - 1.1746n_{\rm f})\ln(u_0)),$$
$$C_T = \frac{1}{u_0^2}(0.0433 - 0.0156n_{\rm f})\ln(u_0),$$

*Supported by the National Natural Science Foundation of China under Grant Nos 11347029 and 11105033.
**Corresponding author. Email: wuliangkai@163.com
© 2017 Chinese Physical Society and IOP Publishing Ltd

with u_0 being $(\langle \mathrm{ReTr}(P)\rangle/3)^{1/4}$.

The Asqtad action is

$$S_{\mathrm{f}} = \langle \Phi | [M^{\dagger}[U]M[U]]^{-n_{\mathrm{f}}/4} | \Phi \rangle,$$

with the form of $M_{x,y}[U] = 2m_{x,y} + D_{x,y}(U)$ reading

$$\begin{aligned} &2m\delta_{x,y} + \sum_{\rho=1,3} \eta_{x,\rho}(U^{F}_{x,\rho}\delta_{x,y-\hat{\rho}} - U^{F\dagger}_{x-\hat{\rho},\rho}\delta_{x,y+\hat{\rho}}) \\ &+ \eta_{x,4}(e^{ia\mu_{\mathrm{I}}}U^{F}_{x,4}\delta_{x,y-\hat{4}} - e^{-ia\mu_{\mathrm{I}}}U^{F\dagger}_{x-\hat{4},\mu}\delta_{x,y+\hat{4}}) \\ &+ \sum_{\rho=1,3} \eta_{x,\rho}(U^{L}_{x,\rho}\delta_{x,y-3\hat{\rho}} - U^{L\dagger}_{x-\rho,\rho}\delta_{x,y+3\hat{\rho}}) \\ &+ \eta_{x,4}(e^{i3a\mu_{\mathrm{I}}}U^{L}_{x,4}\delta_{x,y-3\hat{4}} - e^{-i3a\mu_{\mathrm{I}}}U^{L\dagger}_{x-\hat{4},\mu}\delta_{x,y+3\hat{4}}), \end{aligned}$$

where $U^{F}_{x,\rho}$ stands for the fattened link which is produced by Fat7 smearing, $U^{L}_{x,\rho}$ stands for the Naik term, and $\hat{\rho}$ and $\hat{4}$ are the unit vectors along the ρ-direction, 4-direction, respectively.

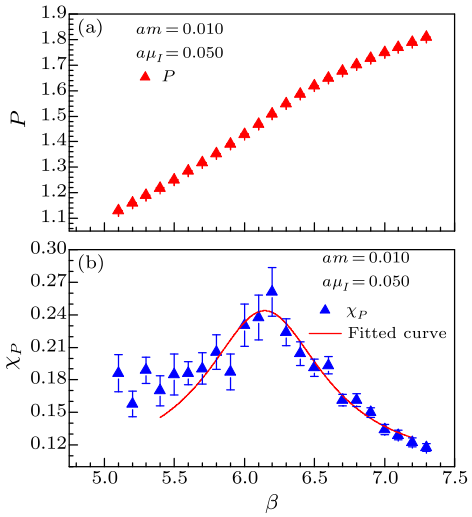

Fig. 1. Values of plaquette (a) and its susceptibility (b) change with β at $a\mu_{\mathrm{I}} = 0.050$. The error of plaquette calculated is so small that the error is hardly discerned. The curve represents the Lorentzian fitting to the susceptibilities.

To probe the transition, we investigate the chiral condensate $\bar{\psi}\psi$, the plaquette variable P, the imaginary part of Polyakov loop $\mathrm{Im}(L)$ and their susceptibilities which are defined as follows:

$$\langle \bar{\psi}\psi \rangle = \frac{N_{\mathrm{f}}}{N_{\mathrm{s}}^3 N_{\mathrm{t}}} \mathrm{Tr}\langle \mathrm{D}^{-1} \rangle,$$

$$\langle L \rangle = \langle \frac{1}{3N_{\mathrm{s}}^3 N_{\mathrm{t}}} \sum_{\mathbf{x}} \mathrm{Tr}[\prod_{t=1}^{N_{\mathrm{t}}} U_4(\mathbf{x}, t)] \rangle,$$

where N_{s} and N_{t} are the spatial, the time extent of lattice, respectively. To simplify the notations, we use X to represent the observables. The susceptibility of one observable is defined as

$$\chi = N_{\mathrm{s}}^3 N_{\mathrm{t}} \langle (X - \langle X \rangle)^2 \rangle.$$

By monitoring the change of χ with β, the location of peak of χ is identified with the transition point.

Before presenting the simulation results, we describe the simulation detail. At quark mass $am = 0.010$, on lattice $12^3 \times 4$, we use one-loop Symanzik-improved gauge action and Asqtad fermion action. The Asqtad action consists of a Fat7 smearing and includes a Naik term. Rational Monte Carlo algorithm [24–26] is used to generate configurations. The Omelyan integration algorithm [27,28] is employed for the gauge and fermion action. The step is chosen to ensure that the acceptance rate is around 87%. Here 5000 trajectories of configuration are taken as warm-up from a cold start, and 20000 trajectories of configuration are updated with 10 trajectories between measurements.

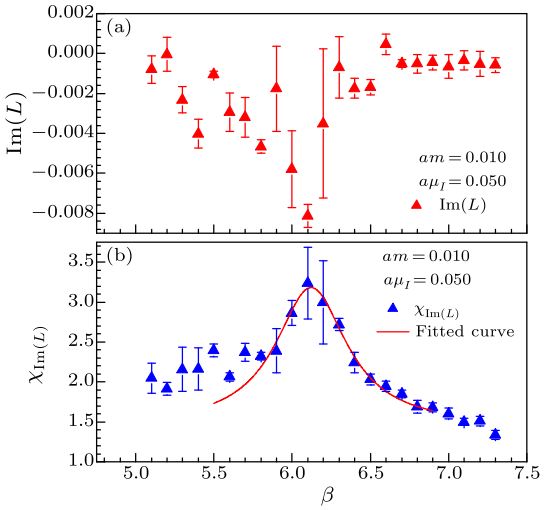

Fig. 2. Values of $\mathrm{Im}(L)$ (a) and its susceptibility (b) change with β at $a\mu_{\mathrm{I}} = 0.050$. The curve represents the Lorentzian fitting to the susceptibilities.

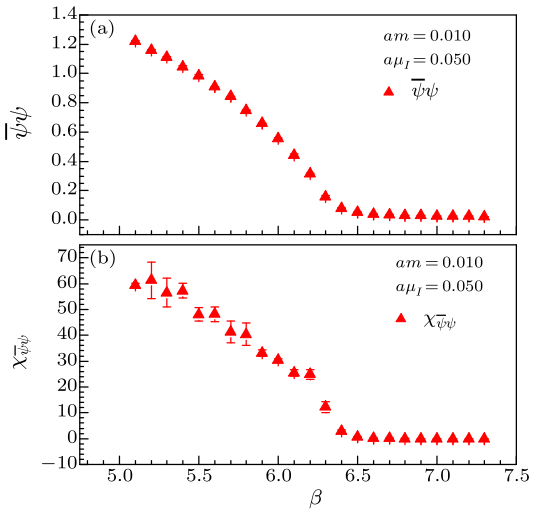

Fig. 3. Values of $\bar{\psi}\psi$ (a) and its susceptibility (b) change with β at $a\mu_{\mathrm{I}} = 0.050$. The error of $\bar{\psi}\psi$ calculated is so small that the error is hardly discerned.

The partition function of QCD with the imaginary chemical potential has two symmetries:[29] reflection symmetry in $i\mu_{\mathrm{I}}$ and periodicity in μ_{I}/T with period $2\pi/3$. We choose μ_{I}/T in the interval $0 < \mu_{\mathrm{I}}/T < \pi/3$. On lattice with $N_{\mathrm{t}} = 4$, the interval $0 < \mu_{\mathrm{I}}/T < \pi/3$ corresponds to the interval $0 < a\mu_{\mathrm{I}} < 0.262$.

We measure $\bar{\psi}\psi$, P, Im(L) and their susceptibilities by scanning β at $a\mu_{\rm I} = 0.050$, 0.150, 0.200, 0.225, 0.250. The values of P, Im(L) and $\bar{\psi}\psi$ at $a\mu_{\rm I} = 0.050$ are presented in Figs. 1–3, respectively. At other values of $a\mu_{\rm I}$, these variables have similar behavior. The Lorentzian fits are performed near the peaks of the susceptibilities for P and Im(L). For clarity, we plot the fitting results at $a\mu_{\rm I} = 0.050$, and 0.250 in Fig. 4.

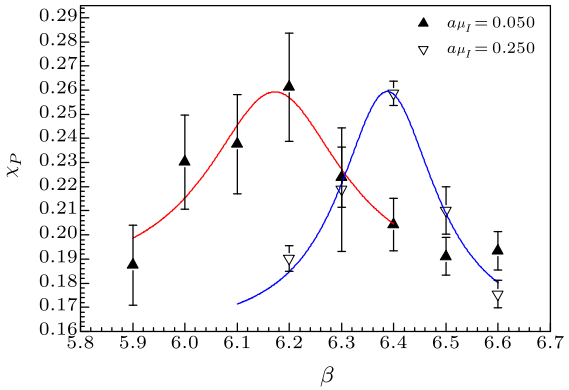

Fig. 4. Only Lorentzian fits to the susceptibilities at $a\mu_{\rm I} = 0.050$ and $a\mu_{\rm I} = 0.250$ are plotted for clarity.

Due to the fact that all the calculations are performed on lattice, the units of variables which have dimension on Figs. 1–5 are measured with the lattice spacing, specifically, $\bar{\psi}\psi$ and $\chi_{\bar{\psi}\psi}$ are with a^3 and a^2, respectively, and the other variables are dimensionless except $a\mu_{\rm I}$ and am which are clearly shown. The fitting results are listed in Table 1.

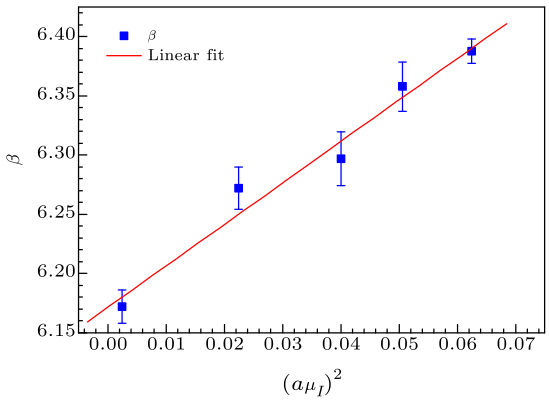

Fig. 5. Linear fit for the critical values of β.

Due to the reflection symmetry at $\mu_{\rm B} = 0$ and analyticity, the transition line $\beta_{\rm c}(a\mu_{\rm I})$ can be expressed as a Taylor series with even power of $a\mu_{\rm I}$. For small $a\mu_{\rm I}$,[30] $\beta_{\rm c}(a\mu_{\rm I})$ can be fitted well by a linear function in $(a\mu_{\rm I}))^2$ by ignoring high-order $(a\mu_{\rm I}))^2$ terms

$$\beta_{\rm c}(a\mu_{\rm I}) = c_0 + c_1(a\mu_{\rm I})^2 + O(a^4\mu_{\rm I}^4). \quad (1)$$

Table 1. Critical β determined by Lorentzian fitting. Here $\beta_{\rm c}(P)$ and $\beta_{\rm c}(L)$ represent β determined from the peaks of χ_P and $\chi_{{\rm Im}(L)}$, respectively.

$a\mu_{\rm I}$	0.050	0.150	0.200	0.225	0.250
$\beta_{\rm c}(P)$	6.172(14)	6.272(18)	6.297(22)	6.357(21)	6.387(10)
$\beta_{\rm c}(L)$	6.223(2)	6.112(20)	6.179(13)	6.234(14)	6.359(16)

Table 2. The values of r_0/a, string tension and pesudoscalar meson mass determined on lattice $12^3 \times 24$. Lattice spacing is extracted with $r_0 = 0.469(7)$ fm.

β	r_0/a	$\sqrt{\sigma}a$	am_π	a (fm)	m_π (MeV)
6.0	1.52(4)	0.546(12)	0.289(2)	0.310(8)	184(5)
6.2	1.78(2)	0.3134(27)	0.293(3)	0.262(2)	219(3)
6.4	2.012(7)	0.2905(11)	0.298(4)	0.2331(7)	251(3)

We use the least square method to fit the data in Table 1. Because the behavior of P is better than the other observables, we use the data from P to fit the pseudo-critical transition line; the fitting range and the line are presented in Fig. 5,

$$\beta_{\rm c} = 6.171(12) + 3.49(27)(a\mu_{\rm I})^2 + O(a^4\mu_{\rm I}^4), \quad (2)$$

with $\chi^2/dof = 0.91$.

Due to the fact that $\beta_{\rm c}(a\mu_{\rm I})$ is an analytic function of $a\mu_{\rm I}$,[30] we can analytically continue from imaginary chemical potential to real one. Replacing $\mu_{\rm I}$ by $-i\mu$ in Eq. (2), we obtain

$$\begin{aligned}\beta_{\rm c}(a\mu) &= c_0 - c_1(a\mu)^2 + O(a^4\mu^4) \\ &= 6.171(12) - 3.49(27)(a\mu_{\rm I})^2 + O(a^4\mu_{\rm I}^4). \quad (3)\end{aligned}$$

To translate our result into a physical unit, we use the two-loop perturbative solution to the renormalization group equation between the lattice spacing a and β,

$$\begin{aligned} a\Lambda_L &= \exp\Big[-\frac{1}{12b_0}\beta + \frac{b_1}{2b_0^2}\ln\Big(\frac{1}{6b_0}\beta\Big)\Big], \\ b_0 &= \frac{1}{16\pi^2}\Big(11 - \frac{2}{3}N_{\rm f}\Big), \\ b_1 &= \Big(\frac{1}{16\pi^2}\Big)^2\Big(102 - \frac{38}{3}N_{\rm f}\Big). \end{aligned}$$

From $T = 1/(aN_{\rm t})$, we obtain

$$\frac{T_{\rm c}(\mu)}{T_{\rm c}(0)} = \frac{a(\beta_{\rm c}(0))\Lambda_L}{a(\beta_{\rm c}(\mu))\Lambda_L}. \quad (4)$$

When we ignore the quark mass dependence in $a(\beta)$, for $n_{\rm f} = 2$, Eq. (4) can be expanded as a function of $\mu_{\rm B}^2$,

$$\frac{T_{\rm c}(\mu_{\rm B})}{T_{\rm c}(\mu_{\rm B} = 0)} = 1 - 0.0326(46)\Big(\frac{\mu_{\rm B}}{T}\Big)^2, \quad (5)$$

where $T_c(\mu_B = 0)$ is set by the critical temperature for two-flavor QCD at $\mu_B = 0$.

To estimate the π meson mass and the lattice spacing a, we carry out the simulation at zero temperature on lattice $12^3 \times 24$ to calculate the heavy quark potential and am_π at $\beta = 6.0$, 6.2 and 6.4. The following expressions are used to extract the lattice spacing a,[31,32]

$$r^2 \frac{dV_{\bar{q}q}(r)}{dr}\Big|_{r=r_0} = 1.65,$$
$$V_{\bar{q}q} = A + B/r + \sigma r.$$

where $r_0 = 0.469(7)$ fm. The results are listed in Table 2.

After the central goal is obtained, some discussions may be in order. Equation (5) shows that the transition temperature T_c decreases with increasing μ_B. This behavior is in accordance with the physical picture. With increasing the baryon density, the interaction between quarks and gluons becomes weaker and thus quark and gluon degrees of freedom become more easily excited, therefore the critical temperature decreases with increasing the baryon chemical potential.

The value of curvature 0.0326(46) is larger than the result obtained in Refs. [12,13]. Qualitatively, our results are consistent with the results obtained in Refs. [5,33], where the values of curvature of 2+1-flavor QCD in the continuum limit are 0.020(4) and 0.0135(20), respectively. This shows that the temperature decreases faster with the increase of the baryon density than the previous results.

It is expedient that we use the two-loop perturbative solution to the renormalization group equation between the lattice spacing a and β to set the scale. The best way out of this is consistent in the nonperturbative determination of the relationship between lattice spacing a and β, which is beyond this study. In addition, a better understanding of the systematic of the lattice determination of curvature requires the extrapolation to the continuum limit.

We thank Philippe de Forcrand and Chuan Liu for valuable assistance. We modify the MILC collaboration's public code [34] to simulate the theory at imaginary chemical potential. This work was carried out at National Supercomputer Center in Wuxi, and we appreciate the help of Qiong Wang and Zhao Liu in carrying out the computation.

References

[1] Ding H T, Karsch F and Mukherjee S 2015 *Int. J. Mod. Phys.* E **24** 1530007
[2] Cleymans J and Redlich K 1998 *Phys. Rev. Lett.* **81** 5284
[3] Hasenfratz P and Karsch F 1983 *Phys. Lett.* B **125** 308
[4] Philipsen O 2006 *PoS LAT* **2005** 016
Schmidt C 2006 *PoS LAT* **2006** 021
De Forcrand P 2009 *PoS LAT* **2009** 010
Aarts G 2012 *PoS LAT* **2012** 017
[5] Cea P, Cosmai L and Papa A 2016 *Phys. Rev.* D **93** 014507
[6] De Forcrand P and Philipsen O 2010 *Phys. Rev. Lett.* **105** 152001
[7] D'Elia M and Sanfilippo F 2009 *Phys. Rev.* D **80** 111501
[8] Bonati C, Cossu G, D'Elia M and Sanfilippo F 2011 *Phys. Rev.* D **83** 054505
[9] Nagata K and Nakamura A 2011 *Phys. Rev.* D **83** 114507
[10] D'Elia M, Di Renzo F and Lombardo M P 2007 *Phys. Rev.* D **76** 114509
[11] De Forcrand P and Philipsen O 2008 *J. High Energy Phys.* **0811** 012
[12] Wu L K, Luo X Q and Chen H C 2007 *Phys. Rev.* D **76** 034505
[13] Wu L K 2010 *Chin. Phys. Lett.* **27** 021101
[14] Symanzik K 1983 *Nucl. Phys.* B **226** 187
[15] Luscher M and Weisz P 1985 *Phys. Lett.* B **158** 250
[16] Lepage G P and Mackenzie P B 1993 *Phys. Rev.* D **48** 2250
[17] Alford M G, Dimm W, Lepage G P, Hockney G and Mackenzie P B 1995 *Phys. Lett.* B **361** 87
[18] Blum T et al 1997 *Phys. Rev.* D **55** R1133
[19] Orginos K et al [MILC Collaboration] 1999 *Phys. Rev.* D **60** 054503
[20] Bazavov A et al 2012 *Phys. Rev.* D **85** 054503
[21] Bazavov A et al [MILC Collaboration] 2010 *Rev. Mod. Phys.* **82** 1349
[22] Naik S 1989 *Nucl. Phys.* B **316** 238
[23] Bernard CW et al [MILC Collaboration] 1998 *Phys. Rev.* D **58** 014503
[24] Clark M A and Kennedy A D 2004 *Nucl. Phys. Proc. Suppl.* **129–130** 850
[25] Clark M A and Kennedy A D 2007 *Phys. Rev.* D **75** 011502
[26] Clark M A and Kennedy A D 2007 *Phys. Rev. Lett.* **98** 051601
[27] Takaishi T and De Forcrand P 2006 *Phys. Rev.* E **73** 036706
[28] Omeylan I P, Mryglod I M and Folk R 2003 *Comp. Phys. Comm.* **151** 272
[29] Roberge A and Weiss N 1986 *Nucl. Phys.* B **275** 734
[30] De Forcrand P and Philipsen O 2002 *Nucl. Phys.* B **642** 290
[31] Sommer R 1994 *Nucl. Phys.* B **411** 839
[32] Cheng M et al 2006 *Phys. Rev.* D **74** 054507
[33] Bonati C, D'Elia M, Mariti M, Mesiti M, Negro F and Sanfilippo F 2015 *Phys. Rev.* D **92** 054503
[34] http://physics.utah.edu/~detar/milc/